
Discovering Structure in High-Dimensional Data Through Correlation Explanation

Greg Ver Steeg
Information Sciences Institute
University of Southern California
Marina del Rey, CA 90292
gregv@isi.edu

Aram Galstyan
Information Sciences Institute
University of Southern California
Marina del Rey, CA 90292
galstyan@isi.edu

Abstract

We introduce a method to learn a hierarchy of successively more abstract representations of complex data based on optimizing an information-theoretic objective. Intuitively, the optimization searches for a set of latent factors that best explain the correlations in the data as measured by multivariate mutual information. The method is unsupervised, requires no model assumptions, and scales linearly with the number of variables which makes it an attractive approach for very high dimensional systems. We demonstrate that Correlation Explanation (CorEx) automatically discovers meaningful structure for data from diverse sources including personality tests, DNA, and human language.

1 Introduction

Without any prior knowledge, what can be automatically learned from high-dimensional data? If the variables are uncorrelated then the system is not really high-dimensional but should be viewed as a collection of unrelated univariate systems. If correlations exist, however, then some common cause or causes must be responsible for generating them. Without assuming any particular model for these hidden common causes, is it still possible to reconstruct them? We propose an information-theoretic principle, which we refer to as “correlation explanation”, that codifies this problem in a model-free, mathematically principled way. Essentially, we are searching for latent factors so that, conditioned on these factors, the correlations in the data are minimized (as measured by multivariate mutual information). In other words, we look for the simplest explanation that accounts for the most correlations in the data. As a bonus, building on this information-based foundation leads naturally to an innovative paradigm for learning hierarchical representations that is more tractable than Bayesian structure learning and provides richer insights than neural network inspired approaches [1].

After introducing the principle of “Correlation Explanation” (CorEx) in Sec. 2, we show that it can be efficiently implemented in Sec. 3. To demonstrate the power of this approach, we begin Sec. 4 with a simple synthetic example and show that standard learning techniques all fail to detect high-dimensional structure while CorEx succeeds. In Sec. 4.2.1, we show that CorEx perfectly reverse engineers the “big five” personality types from survey data while other approaches fail to do so. In Sec. 4.2.2, CorEx automatically discovers in DNA nearly perfect predictors of independent signals relating to gender, geography, and ethnicity. In Sec. 4.2.3, we apply CorEx to text and recover both stylistic features and hierarchical topic representations. After briefly considering intriguing theoretical connections in Sec. 5, we conclude with future directions in Sec. 6.

2 Correlation Explanation

Using standard notation [2], capital X denotes a discrete random variable whose instances are written in lowercase. A probability distribution over a random variable X , $p_X(X = x)$, is shortened

to $p(x)$ unless ambiguity arises. The cardinality of the set of values that a random variable can take will always be finite and denoted by $|X|$. If we have n random variables, then G is a subset of indices $G \subseteq \mathbb{N}_n = \{1, \dots, n\}$ and X_G is the corresponding subset of the random variables ($X_{\mathbb{N}_n}$ is shortened to X). Entropy is defined in the usual way as $H(X) \equiv \mathbb{E}_X[-\log p(x)]$. Higher-order entropies can be constructed in various ways from this standard definition. For instance, the mutual information between two random variables, X_1 and X_2 can be written $I(X_1 : X_2) = H(X_1) + H(X_2) - H(X_1, X_2)$.

The following measure of mutual information among many variables was first introduced as “total correlation” [3] and is also called multi-information [4] or multivariate mutual information [5].

$$TC(X_G) = \sum_{i \in G} H(X_i) - H(X_G) \quad (1)$$

For $G = \{i_1, i_2\}$, this corresponds to the mutual information, $I(X_{i_1} : X_{i_2})$. $TC(X_G)$ is non-negative and zero if and only if the probability distribution factorizes. In fact, total correlation can also be written as a KL divergence, $TC(X_G) = D_{KL}(p(x_G) || \prod_{i \in G} p(x_i))$.

The total correlation among a group of variables, X , after conditioning on some other variable, Y , is simply $TC(X|Y) = \sum_i H(X_i|Y) - H(X|Y)$. We can measure the extent to which Y explains the correlations in X by looking at how much the total correlation is reduced.

$$TC(X; Y) \equiv TC(X) - TC(X|Y) = \sum_{i \in \mathbb{N}_n} I(X_i : Y) - I(X : Y) \quad (2)$$

We use semicolons as a reminder that $TC(X; Y)$ is not symmetric in the arguments, unlike mutual information. $TC(X|Y)$ is zero (and $TC(X; Y)$ maximized) if and only if the distribution of X 's conditioned on Y factorizes. This would be the case if Y were the common cause of all the X_i 's in which case Y explains all the correlation in X . $TC(X_G|Y) = 0$ can also be seen as encoding local Markov properties among a group of variables and, therefore, specifying a DAG [6]. This quantity has appeared as a measure of the *redundant* information that the X_i 's carry about Y [7]. More connections are discussed in Sec. 5.

Optimizing over Eq. 2 can now be seen as a search for a latent factor, Y , that explains the correlations in X . We can make this concrete by letting Y be a discrete random variable that can take one of k possible values and searching over all probabilistic functions of X , $p(y|x)$.

$$\max_{p(y|x)} TC(X; Y) \quad \text{s.t.} \quad |Y| = k, \quad (3)$$

The solution to this optimization is given as a special case in Sec. A. Total correlation is a functional over the joint distribution, $p(x, y) = p(y|x)p(x)$, so the optimization implicitly depends on the data through $p(x)$. Typically, we have only a small number of samples drawn from $p(x)$ (compared to the size of the state space). To make matters worse, if $x \in \{0, 1\}^n$ then optimizing over all $p(y|x)$ involves at least 2^n variables. Surprisingly, despite these difficulties we show in the next section that this optimization can be carried out efficiently. The maximum achievable value of this objective occurs for some finite k when $TC(X|Y) = 0$. This implies that the data are perfectly described by a naive Bayes model with Y as the parent and X_i as the children.

Generally, we expect that correlations in data may result from several different factors. Therefore, we extend the optimization above to include m different factors, Y_1, \dots, Y_m .¹

$$\max_{G_j, p(y_j|x_{G_j})} \sum_{j=1}^m TC(X_{G_j}; Y_j) \quad \text{s.t.} \quad |Y_j| = k, G_j \cap G_{j' \neq j} = \emptyset \quad (4)$$

Here we simultaneously search subsets of variables G_j and over variables Y_j that explain the correlations in each group. While it is not necessary to make the optimization tractable, we impose an additional condition on G_j so that each variable X_i is in a single group, G_j , associated with a single “parent”, Y_j . The reason for this restriction is that it has been shown that the value of the objective can then be interpreted as a lower bound on $TC(X)$ [8]. Note that this objective is valid

¹Note that in principle we could have just replaced Y in Eq. 3 with (Y_1, \dots, Y_m) , but the state space would have been exponential in m , leading to an intractable optimization.

and meaningful regardless of details about the data-generating process. We only assume that we are given $p(x)$ or iid samples from it.

The output of this procedure gives us Y_j 's, which are probabilistic functions of X . If we iteratively apply this optimization to the resulting probability distribution over Y by searching for some $Z_1, \dots, Z_{\bar{m}}$ that explain the correlations in the Y 's, we will end up with a hierarchy of variables that forms a tree. We now show that the optimization in Eq. 4 can be carried out efficiently even for high-dimensional spaces and small numbers of samples.

3 CorEx: Efficient Implementation of Correlation Explanation

We begin by re-writing the optimization in Eq. 4 in terms of mutual informations using Eq. 2.

$$\max_{G, p(y_j|x)} \sum_{j=1}^m \sum_{i \in G_j} I(Y_j : X_i) - \sum_{j=1}^m I(Y_j : X_{G_j}) \quad (5)$$

Next, we replace G with a set indicator variable, $\alpha_{i,j} = \mathbb{I}[X_i \in G_j] \in \{0, 1\}$.

$$\max_{\alpha, p(y_j|x)} \sum_{j=1}^m \sum_{i=1}^n \alpha_{i,j} I(Y_j : X_i) - \sum_{j=1}^m I(Y_j : X) \quad (6)$$

The non-overlapping group constraint is enforced by demanding that $\sum_{\bar{j}} \alpha_{i,\bar{j}} = 1$. Note also that we dropped the subscript G_j in the second term of Eq. 6 but this has no effect because solutions must satisfy $I(Y_j : X) = I(Y_j : X_{G_j})$, as we now show.

For fixed α , it is straightforward to find the solution of the Lagrangian optimization problem as the solution to a set of self-consistent equations. Details of the derivation can be found in Sec. A.

$$p(y_j|x) = \frac{1}{Z_j(x)} p(y_j) \prod_{i=1}^n \left(\frac{p(y_j|x_i)}{p(y_j)} \right)^{\alpha_{i,j}} \quad (7)$$

$$p(y_j|x_i) = \sum_{\bar{x}} p(y_j|\bar{x}) p(\bar{x}) \delta_{\bar{x}, x_i} / p(x_i) \text{ and } p(y_j) = \sum_{\bar{x}} p(y_j|\bar{x}) p(\bar{x}) \quad (8)$$

Note that δ is the Kronecker delta and that Y_j depends only on the X_i for which $\alpha_{i,j}$ is non-zero. Remarkably, Y_j 's dependence on X can be written in terms of a *linear* (in n , the number of variables) number of parameters which are just the marginals, $p(y_j), p(y_j|x_i)$. We approximate $p(x)$ with the empirical distribution, $\hat{p}(\bar{x}) = \sum_{l=1}^N \delta_{\bar{x}, x^{(l)}} / N$. This approximation allows us to estimate marginals with fixed accuracy using only a constant number of iid samples from the true distribution. In Sec. A we show that Eq. 7, which defines the soft labeling of any x , can be seen as a linear function followed by a non-linear threshold, reminiscent of neural networks. Also note that the normalization constant for any x , $Z_j(x)$, can be calculated easily by summing over just $|Y_j| = k$ values.

For fixed values of the parameters $p(y_j|x_i)$, we have an integer linear program for α made easy by the constraint $\sum_{\bar{j}} \alpha_{i,\bar{j}} = 1$. The solution is $\alpha_{i,j}^* = \mathbb{I}[j = \arg \max_{\bar{j}} I(X_i : Y_{\bar{j}})]$. However, this leads to a rough optimization space. The solution in Eq. 7 is valid (and meaningful, see Sec. 5 and [8]) for arbitrary values of α so we relax our optimization accordingly. At step $t = 0$ in the optimization, we pick $\alpha_{i,j}^{t=0} \sim \mathcal{U}(1/2, 1)$ uniformly at random (violating the constraints). At step $t + 1$, we make a small update on α in the direction of the solution.

$$\alpha_{i,j}^{t+1} = (1 - \lambda) \alpha_{i,j}^t + \lambda \alpha_{i,j}^{**} \quad (9)$$

The second term, $\alpha_{i,j}^{**} = \exp(\gamma(I(X_i : Y_j) - \max_{\bar{j}} I(X_i : Y_{\bar{j}})))$, implements a soft-max which converges to the true solution for α^* in the limit $\gamma \rightarrow \infty$. This leads to a smooth optimization and good choices for λ, γ can be set through intuitive arguments described in Sec. B.

Now that we have rules to update both α and $p(y_j|x_i)$ to increase the value of the objective, we simply iterate between them until we achieve convergence. While there is no guarantee to find the global optimum, the objective is upper bounded by $TC(X)$ (or equivalently, $TC(X|Y)$ is lower bounded by 0). Pseudo-code for this approach is described in Algorithm 1 with additional details provided in Sec. B and source code available online². The overall complexity is linear in the number

²Open source code is available at <http://github.com/gregversteeg/CorEx>.

```

input : A matrix of size  $n_s \times n$  representing  $n_s$  samples of  $n$  discrete random variables
set : Set  $m$ , the number of latent variables,  $Y_j$ , and  $k$ , so that  $|Y_j| = k$ 
output: Parameters  $\alpha_{i,j}, p(y_j|x_i), p(y_j), p(y|x^{(l)})$ 
         for  $i \in \mathbb{N}_n, j \in \mathbb{N}_m, l \in \mathbb{N}_{n_s}, y \in \mathbb{N}_k, x_i \in \mathcal{X}_i$ 

Randomly initialize  $\alpha_{i,j}, p(y|x^{(l)})$ ;
repeat
  Estimate marginals,  $p(y_j), p(y_j|x_i)$  using Eq. 8;
  Calculate  $I(X_i : Y_j)$  from marginals;
  Update  $\alpha$  using Eq. 9;
  Calculate  $p(y|x^{(l)}), l = 1, \dots, n_s$  using Eq. 7;
until convergence;

```

Algorithm 1: Pseudo-code implementing Correlation Explanation (CorEx)

of variables. To bound the complexity in terms of the number of samples, we can always use mini-batches of fixed size to estimate the marginals in Eq. 8.

A common problem in representation learning is how to pick m , the number of latent variables to describe the data. Consider the limit in which we set $m = n$. To use all Y_1, \dots, Y_m in our representation, we would need exactly one variable, X_i , in each group, G_j . Then $\forall j, TC(X_{G_j}) = 0$ and, therefore, the whole objective will be 0. This suggests that the maximum value of the objective must be achieved for some value of $m < n$. In practice, this means that if we set m too high, only some subset of latent variables will be used in the solution, as we will demonstrate in Fig. 2. In other words, if m is set high enough, the optimization will result in some number of clusters $m' < m$ that is optimal with respect to the objective. Representations with different numbers of layers, different m , and different k can be compared according to how tight of a lower bound they provide on $TC(X)$ [8].

4 Experiments

4.1 Synthetic data

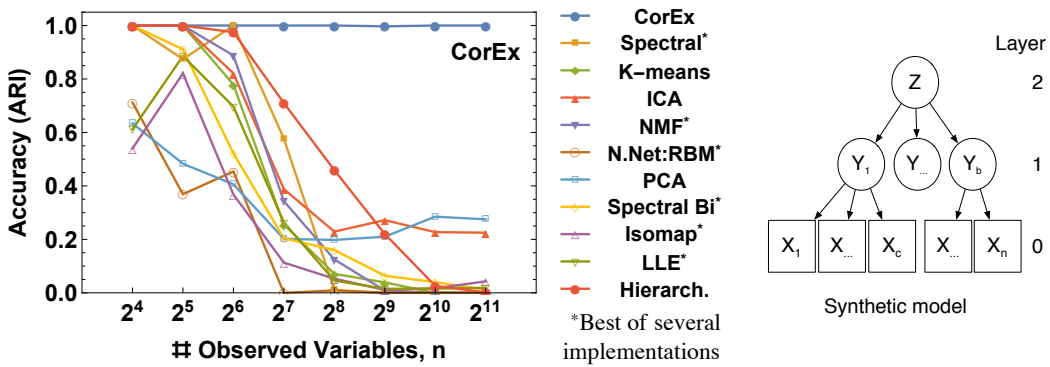


Figure 1: (Left) We compare methods to recover the clusters of variables generated according to the model. (Right) Synthetic data is generated according to a tree of latent variables.

To test CorEx’s ability to recover latent structure from data we begin by generating synthetic data according to the latent tree model depicted in Fig. 1 in which all the variables are hidden except for the leaf nodes. The most difficult part of reconstructing this tree is clustering of the leaf nodes. If a clustering method can do that then the latent variables can be reconstructed for each cluster easily using EM. We consider many different clustering methods, typically with several variations

of each technique, details of which are described in Sec. C. We use the adjusted Rand index (ARI) to measure the accuracy with which inferred clusters recover the ground truth.³

We generated samples from the model in Fig. 1 with $b = 8$ and varied c , the number of leaves per branch. The X_i 's depend on Y_j 's through a binary erasure channel (BEC) with erasure probability δ . The capacity of the BEC is $1 - \delta$ so we let $\delta = 1 - 2/c$ to reflect the intuition that the signal from each parent node is weakly distributed across all its children (but cannot be inferred from a single child). We generated $\max(200, 2n)$ samples. In this example, all the Y_j 's are weakly correlated with the root node, Z , through a binary symmetric channel with flip probability of $1/3$.

Fig. 1 shows that for a small to medium number of variables, all the techniques recover the structure fairly well, but as the dimensionality increases only CorEx continues to do so. ICA and hierarchical clustering compete for second place. CorEx also perfectly recovers the values of the latent factors in this example. For latent tree models, recovery of the latent factors gives a global optimum of the objective in Eq. 4. Even though CorEx is only guaranteed to find local optima, in this example it correctly converges to the global optimum over a range of problem sizes.

Note that a growing literature on latent tree learning attempts to reconstruct latent trees with theoretical guarantees [9, 10]. In principle, we should compare to these techniques, but they scale as $O(n^2) - O(n^5)$ (see [31], Table 1) while our method is $O(n)$. In a recent survey on latent tree learning methods, only one out of 15 techniques was able to run on the largest dataset considered (see [31], Table 3), while most of the datasets in this paper are orders of magnitude larger than that one.

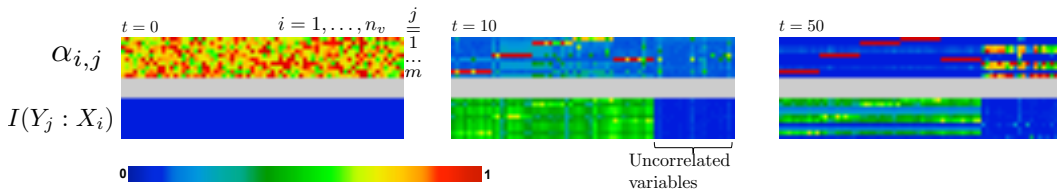


Figure 2: (Color online) A visualization of structure learning in CorEx, see text for details.

Fig. 2 visualizes the structure learning process.⁴ This example is similar to that above but includes some uncorrelated random variables to show how they are treated by CorEx. We set $b = 5$ clusters of variables but we used $m = 10$ hidden variables. At each iteration, t , we show which hidden variables, Y_j , are connected to input variables, X_i , through the connectivity matrix, α (shown on top). The mutual information is shown on the bottom. At the beginning, we started with full connectivity, but with nothing learned we have $I(Y_j : X_i) = 0$. Over time, the hidden units “compete” to find a group of X_i 's for which they can explain all the correlations. After only ten iterations the overall structure appears and by 50 iterations it is exactly described. At the end, the uncorrelated random variables (X_i 's) and the hidden variables (Y_j 's) which have not explained any correlations can be easily distinguished and discarded (visually and mathematically, see Sec. B).

4.2 Discovering Structure in Diverse Real-World Datasets

4.2.1 Personality Surveys and the “Big Five” Personality Traits

One psychological theory suggests that there are five traits that largely reflect the differences in personality types [11]: *extraversion*, *neuroticism*, *agreeableness*, *conscientiousness* and *openness to experience*. Psychologists have designed various instruments intended to measure whether individuals exhibit these traits. We consider a survey in which subjects rate fifty statements, such as, “I am the life of the party”, on a five point scale: (1) disagree, (2) slightly disagree, (3) neutral, (4) slightly agree, and (5) agree.⁵ The data consist of answers to these questions from about ten

³Rand index counts the percentage of pairs whose relative classification matches in both clusterings. ARI adds a correction so that a random clustering will give a score of zero, while an ARI of 1 corresponds to a perfect match.

⁴A video is available online at http://isi.edu/~gregv/corex_structure.mpg.

⁵Data and full list of questions are available at http://personality-testing.info/_rawdata/.

thousand test-takers. The test was designed with the intention that each question should belong to a cluster according to which personality trait the question gauges. Is it true that there are five factors that strongly predict the answers to these questions?

CorEx learned a two-level hierarchical representation when applied to this data (full model shown in Fig. C.2). On the first level, CorEx automatically determined that the questions should cluster into five groups. Surprisingly, the five clusters *exactly* correspond to the big five personality traits as labeled by the test designers. It is unusual to recover the ground truth with perfect accuracy on an unsupervised learning problem so we tried a number of other standard clustering methods to see if they could reproduce this result. We display the results using confusion matrices in Fig. 3. The details of the techniques used are described in Sec. C but all of them had an advantage over CorEx since they required that we specify the correct number of clusters. None of the other techniques are able to recover the five personality types exactly.

Interestingly, Independent Component Analysis (ICA) [12] is the only other method that comes close. The intuition behind ICA is that it find a linear transformation on the input that minimizes the multi-information among the outputs (Y_j). In contrast, CorEx searches for Y_j 's so that multi-information among the X_i 's is minimized after conditioning on Y . ICA assumes that the signals that give rise to the data are independent while CorEx does not. In this case, personality traits like “extraversion” and “agreeableness” are correlated, violating the independence assumption.

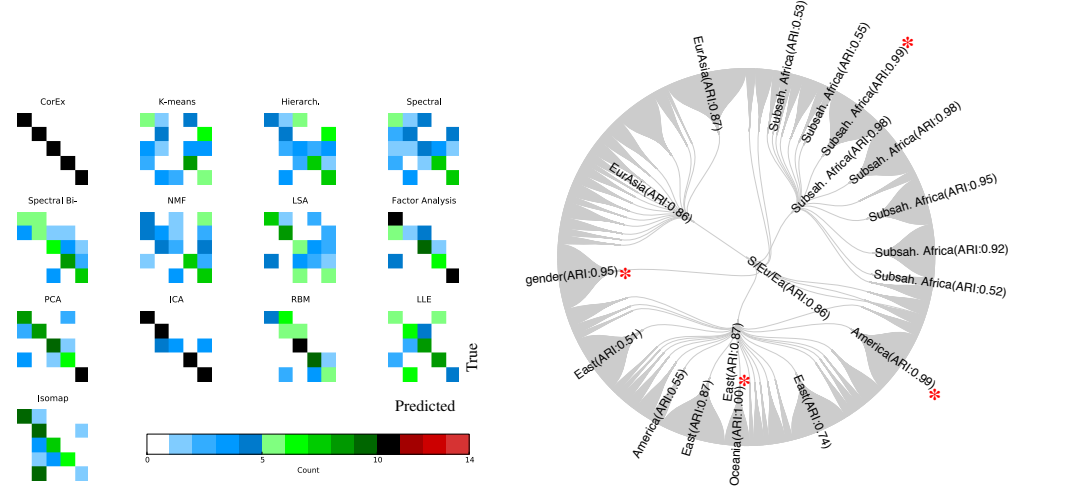


Figure 3: (Left) Confusion matrix comparing predicted clusters to true clusters for the questions on the Big-5 personality test. (Right) Hierarchical model constructed from samples of DNA by CorEx.

4.2.2 DNA from the Human Genome Diversity Project

Next, we consider DNA data taken from 952 individuals of diverse geographic and ethnic backgrounds [13]. The data consist of 4170 variables describing different SNPs (single nucleotide polymorphisms).⁶ We use CorEx to learn a hierarchical representation which is depicted in Fig. 3. To evaluate the quality of the representation, we use the adjusted Rand index (ARI) to compare clusters induced by each latent variable in the hierarchical representation to different demographic variables in the data. Latent variables which substantially match demographic variables are labeled in Fig. 3.

The representation learned (*unsupervised*) on the first layer contains a perfect match for Oceania (the Pacific Islands) and nearly perfect matches for America (Native Americans), Sub-Saharan Africa, and gender. The second layer has three variables which correspond very closely to broad geographic regions: Sub-Saharan Africa, the “East” (including China, Japan, Oceania, America), and EurAsia.

4.2.3 Text from the Twenty Newsgroups Dataset

The twenty newsgroups dataset consists of documents taken from twenty different topical message boards with about a thousand posts each [14]. For analyzing unstructured text, typical feature en-

⁶Data, descriptions of SNPs, and detailed demographics of subjects is available at ftp://ftp.cephb.fr/hgdp_v3/.

gineering approaches heuristically separate signals like style, sentiment, or topics. In principle, all three of these signals manifest themselves in terms of subtle correlations in word usage. Recent attempts at learning large-scale unsupervised hierarchical representations of text have produced interesting results [15], though validation is difficult because quantitative measures of representation quality often do not correlate well with human judgment [16].

To focus on linguistic signals, we removed meta-data like headers, footers, and replies even though these give strong signals for supervised newsgroup classification. We considered the top ten thousand most frequent tokens and constructed a bag of words representation. Then we used CorEx to learn a five level representation of the data with 326 latent variables in the first layer. Details are described in Sec. C.1. Portions of the first three levels of the tree keeping only nodes with the highest normalized mutual information with their parents are shown in Fig. 4 and in Fig. C.1.⁷

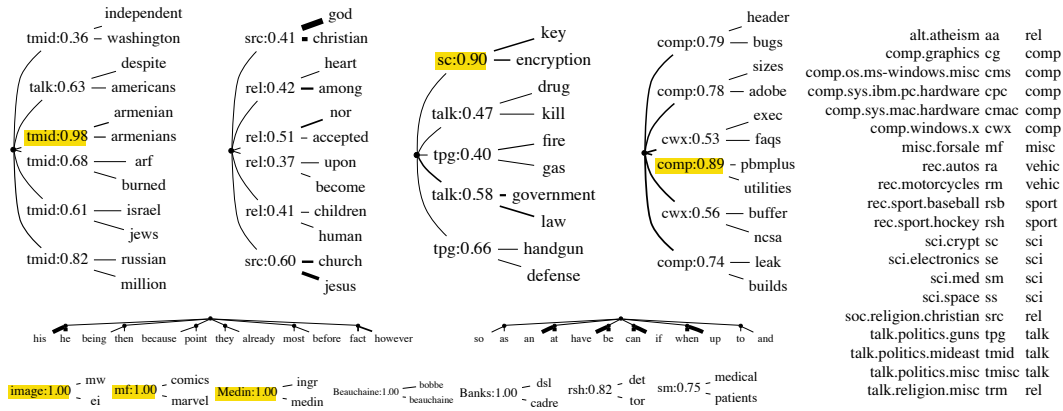


Figure 4: Portions of the hierarchical representation learned for the twenty newsgroups dataset. We label latent variables that overlap significantly with known structure. Newsgroup names, abbreviations, and broad groupings are shown on the right.

To provide a more quantitative benchmark of the results, we again test to what extent learned representations are related to known structure in the data. Each post can be labeled by the newsgroup it belongs to, according to broad categories (e.g. groups that include “comp”), or by author. Most learned binary variables were active in around 1% of the posts, so we report the fraction of activations that coincide with a known label (precision) in Fig. 4. Most variables clearly represent sub-topics of the newsgroup topics, so we do not expect high recall. The small portion of the tree shown in Fig. 4 reflects intuitive relationships that contain hierarchies of related sub-topics as well as clusters of function words (e.g. pronouns like “he/his/him” or tense with “have/be”).

Once again, several learned variables perfectly captured known structure in the data. Some users sent images in text using an encoded format. One feature matched all the image posts (with perfect precision and recall) due to the correlated presence of unusual short tokens. There were also perfect matches for three frequent authors: G. Banks, D. Medin, and B. Beauchaine. Note that the learned variables did not trigger if just their names appeared in the text, but only for posts they authored. These authors had elaborate signatures with long, identifiable quotes that evaded pre-processing but created a strongly correlated signal. Another variable with perfect precision for the “forsale” newsgroup labeled comic book sales (but did not activate for discussion of comics in other newsgroups). Other nearly perfect predictors described extensive discussions of Armenia/Turkey in *talk.politics.mideast* (a fifth of all discussion in that group), specialized unix jargon, and a match for *sci.crypt* which had 90% precision and 55% recall. When we ranked all the latent factors according to a normalized version of Eq. 2, these examples all showed up in the top 20.

5 Connections and Related Work

While the basic measures used in Eq. 1 and Eq. 2 have appeared in several contexts [7, 17, 4, 3, 18], the interpretation of these quantities is an active area of research [19, 20]. The optimizations we

⁷An interactive tool for exploring the full hierarchy is available at <http://bit.ly/corexvis>.

define have some interesting but less obvious connections. For instance, the optimization in Eq. 3 is similar to one recently introduced as a measure of “common information” [21]. The objective in Eq. 6 (for a single Y_j) appears exactly as a bound on “ancestral” information [22]. For instance, if all the $\alpha_i = 1/\beta$ then Steudel and Ay [22] show that the objective is positive only if at least $1 + \beta$ variables share a common ancestor in any DAG describing them. This provides extra rationale for relaxing our original optimization to include non-binary values of $\alpha_{i,j}$.

The most similar learning approach to the one presented here is the information bottleneck [23] and its extension the multivariate information bottleneck [24, 25]. The motivation behind information bottleneck is to compress the data (X) into a smaller representation (Y) so that information about some relevance term (typically labels in a supervised learning setting) is maintained. The second term in Eq. 6 is analogous to the compression term. Instead of maximizing a relevance term, we are maximizing information about all the individual sub-systems of X , the X_i . The most redundant information in the data is preferentially stored while uncorrelated random variables are completely ignored.

The broad problem of transforming complex data into simpler, more meaningful forms goes under the rubric of *representation learning* [26] which shares many goals with dimensionality reduction and subspace clustering. Insofar as our approach learns a hierarchy of representations it superficially resembles “deep” approaches like neural nets and autoencoders [27, 28, 29, 30]. While those approaches are scalable, a common critique is that they involve many heuristics discovered through trial-and-error that are difficult to justify. On the other hand, a rich literature on learning latent tree models [31, 32, 9, 10] have excellent theoretical properties but do not scale well. By basing our method on an information-theoretic optimization that can nevertheless be performed quite efficiently, we hope to preserve the best of both worlds.

6 Conclusion

The most challenging open problems today involve high-dimensional data from diverse sources including human behavior, language, and biology.⁸ The complexity of the underlying systems makes modeling difficult. We have demonstrated a model-free approach to learn successfully more coarse-grained representations of complex data by efficiently optimizing an information-theoretic objective. The principle of explaining as much correlation in the data as possible provides an intuitive and fully data-driven way to discover previously inaccessible structure in high-dimensional systems.

It may seem surprising that CorEx should perfectly recover structure in diverse domains without using labeled data or prior knowledge. On the other hand, the patterns discovered are “low-hanging fruit” from the right point of view. Intelligent systems should be able to learn robust and general patterns in the face of rich inputs even in the absence of labels to define what is important. Information that is very redundant in high-dimensional data provides a good starting point.

Several fruitful directions stand out. First, the promising preliminary results invite in-depth investigations on these and related problems. From a computational point of view, the main work of the algorithm involves a matrix multiplication followed by an element-wise non-linear transform. The same is true for neural networks and they have been scaled to very large data using, e.g., GPUs. On the theoretical side, generalizing this approach to allow non-tree representations appears both feasible and desirable [8].

Acknowledgments

We thank Virgil Griffith, Shuyang Gao, Hsuan-Yi Chu, Shirley Pepke, Bilal Shaw, Jose-Luis Ambite, and Nathan Hodas for helpful conversations. This research was supported in part by AFOSR grant FA9550-12-1-0417 and DARPA grant W911NF-12-1-0034.

References

- [1] C. Szegedy, W. Zaremba, I. Sutskever, J. Bruna, D. Erhan, I. Goodfellow, and R. Fergus. Intriguing properties of neural networks. In *ICLR*, 2014.

⁸In principle, computer vision should be added to this list. However, the success of unsupervised feature learning with neural nets for vision appears to rely on encoding generic priors about vision through heuristics like convolutional coding and max pooling [33]. Since CorEx is a knowledge-free method it will perform relatively poorly unless we find a way to also encode these assumptions.

- [2] Thomas M Cover and Joy A Thomas. *Elements of information theory*. Wiley-Interscience, 2006.
- [3] Satoshi Watanabe. Information theoretical analysis of multivariate correlation. *IBM Journal of research and development*, 4(1):66–82, 1960.
- [4] M Studený and J Vejnarova. The multiinformation function as a tool for measuring stochastic dependence. In *Learning in graphical models*, pages 261–297. Springer, 1998.
- [5] Alexander Kraskov, Harald Stögbauer, Ralph G Andrzejak, and Peter Grassberger. Hierarchical clustering using mutual information. *EPL (Europhysics Letters)*, 70(2):278, 2005.
- [6] J. Pearl. *Causality: Models, Reasoning and Inference*. Cambridge University Press, NY, NY, USA, 2009.
- [7] Elad Schneidman, William Bialek, and Michael J Berry. Synergy, redundancy, and independence in population codes. *the Journal of Neuroscience*, 23(37):11539–11553, 2003.
- [8] Greg Ver Steeg and Aram Galstyan. Maximally informative hierarchical representations of high-dimensional data. *arXiv:1410.7404*, 2014.
- [9] Animashree Anandkumar, Kamalika Chaudhuri, Daniel Hsu, Sham M Kakade, Le Song, and Tong Zhang. Spectral methods for learning multivariate latent tree structure. In *NIPS*, pages 2025–2033, 2011.
- [10] Myung Jin Choi, Vincent YF Tan, Animashree Anandkumar, and Alan S Willsky. Learning latent tree graphical models. *The Journal of Machine Learning Research*, 12:1771–1812, 2011.
- [11] Lewis R Goldberg. The development of markers for the big-five factor structure. *Psychological assessment*, 4(1):26, 1992.
- [12] Aapo Hyvärinen and Erkki Oja. Independent component analysis: algorithms and applications. *Neural networks*, 13(4):411–430, 2000.
- [13] N.A. Rosenberg, J.k. Pritchard, J.L. Weber, H.M. Cann, K.K. Kidd, L.A. Zhivotovsky, and M.W. Feldman. Genetic structure of human populations. *Science*, 298(5602):2381–2385, 2002.
- [14] K. Bache and M. Lichman. UCI machine learning repository, 2013.
- [15] Tomas Mikolov, Kai Chen, Greg Corrado, and Jeffrey Dean. Efficient estimation of word representations in vector space. *arXiv:1301.3781*, 2013.
- [16] Jonathan Chang, Jordan L Boyd-Graber, Sean Gerrish, Chong Wang, and David M Blei. Reading tea leaves: How humans interpret topic models. In *NIPS*, volume 22, pages 288–296, 2009.
- [17] Elad Schneidman, Susanne Still, Michael J Berry, William Bialek, et al. Network information and connected correlations. *Physical Review Letters*, 91(23):238701, 2003.
- [18] Nihat Ay, Eckehard Olbrich, Nils Bertschinger, and Jürgen Jost. A unifying framework for complexity measures of finite systems. *Proceedings of European Complex Systems Society*, 2006.
- [19] P.L. Williams and R.D. Beer. Nonnegative decomposition of multivariate information. *arXiv:1004.2515*, 2010.
- [20] Virgil Griffith and Christof Koch. Quantifying synergistic mutual information. *arXiv:1205.4265*, 2012.
- [21] Gowtham Ramani Kumar, Cheuk Ting Li, and Abbas El Gamal. Exact common information. *arXiv:1402.0062*, 2014.
- [22] B. Steudel and N. Ay. Information-theoretic inference of common ancestors. *arXiv:1010.5720*, 2010.
- [23] Naftali Tishby, Fernando C Pereira, and William Bialek. The information bottleneck method. *arXiv:physics/0004057*, 2000.
- [24] Noam Slonim, Nir Friedman, and Naftali Tishby. Multivariate information bottleneck. *Neural Computation*, 18(8):1739–1789, 2006.
- [25] Noam Slonim. *The information bottleneck: Theory and applications*. PhD thesis, Citeseer, 2002.
- [26] Yoshua Bengio, Aaron Courville, and Pascal Vincent. Representation learning: A review and new perspectives. *Pattern Analysis and Machine Intelligence, IEEE Transactions on*, 35(8):1798–1828, 2013.
- [27] Geoffrey E Hinton and Ruslan R Salakhutdinov. Reducing the dimensionality of data with neural networks. *Science*, 313(5786):504–507, 2006.
- [28] Yann LeCun, Léon Bottou, Yoshua Bengio, and Patrick Haffner. Gradient-based learning applied to document recognition. *Proceedings of the IEEE*, 86(11):2278–2324, 1998.
- [29] Yann LeCun and Yoshua Bengio. Convolutional networks for images, speech, and time series. *The handbook of brain theory and neural networks*, 3361, 1995.
- [30] Yoshua Bengio, Pascal Lamblin, Dan Popovici, and Hugo Larochelle. Greedy layer-wise training of deep networks. *Advances in neural information processing systems*, 19:153, 2007.
- [31] Raphaël Mourad, Christine Sinoquet, Nevin L Zhang, Tengfei Liu, Philippe Leray, et al. A survey on latent tree models and applications. *J. Artif. Intell. Res.(JAIR)*, 47:157–203, 2013.

- [32] Ryan Prescott Adams, Hanna M Wallach, and Zoubin Ghahramani. Learning the structure of deep sparse graphical models. *arXiv:1001.0160*, 2009.
- [33] H. Lee, R. Grosse, R. Ranganath, and A. Ng. Convolutional deep belief networks for scalable unsupervised learning of hierarchical representations. In *ICML*, 2009.
- [34] F. Pedregosa, G. Varoquaux, A. Gramfort, V. Michel, B. Thirion, O. Grisel, M. Blondel, P. Prettenhofer, R. Weiss, V. Dubourg, J. Vanderplas, A. Passos, D. Cournapeau, M. Brucher, M. Perrot, and E. Duchesnay. Scikit-learn: Machine learning in Python. *Journal of Machine Learning Research*, 12:2825–2830, 2011.

Supplementary Material for “Discovering Structure in High-Dimensional Data Through Correlation Explanation”

A Derivation of Eqs. 7 and 8

We want to optimize the following objective.

$$\begin{aligned} \max_{\alpha, p(y_j|x)} \quad & \sum_{j=1}^m \sum_{i=1}^n \alpha_{i,j} I(Y_j : X_i) - \sum_{j=1}^m I(Y_j : X) \\ \text{s.t.} \quad & \sum_{y_j} p(y_j|x) = 1 \end{aligned} \tag{10}$$

In principle, we would also like $\forall i, j, \alpha_{i,j} \in \{0, 1\}, \sum_{\bar{j}} \alpha_{i,\bar{j}} = 1$, but we begin by solving the optimization for fixed α .

We proceed using Lagrangian optimization. We introduce a Lagrange multiplier $\lambda_j(x)$ for each value of x and each j to enforce the normalization constraint and then reduce the constrained optimization problem to the unconstrained optimization of the objective $\mathcal{L}_{tot} = \sum_j \mathcal{L}_j$. We show the solution for a single \mathcal{L}_j , but drop the j index to avoid clutter. (For fixed α , the optimization for different j totally decouple.)

$$\begin{aligned} \mathcal{L} = \sum_{x,y} p(x)p(y|x) & \left(\sum_i \alpha_i (\log p(y|x_i) - \log(p(y))) - (\log p(y|x) - \log(p(y))) \right) \\ & + \sum_x \lambda(x) \left(\sum_y p(y|x) - 1 \right) \end{aligned}$$

Note that we are optimizing over $p(y|x)$ and so the marginals $p(y|x_i), p(y)$ are actually linear functions of $p(y|x)$. Next we take the functional derivatives with respect to $p(y|x)$ and set them equal to 0. Note that this can be done symbolically and proceeds in similar fashion to the detailed calculations of information bottleneck [25].

This leads to the following condition.

$$p(y_j|x) = \frac{1}{Z(x)} p(y_j) \prod_{i=1}^n \left(\frac{p(y_j|x_i)}{p(y_j)} \right)^{\alpha_{i,j}}$$

But this is only a formal solution since the marginals themselves are defined in terms of $p(y|x)$.

$$p(y) = \sum_x p(x)p(y|x), \quad p(y|x_i) = \sum_{x_j \neq i} p(y|x)p(x)/p(x_i)$$

The partition constant, $Z(x)$ can be easily calculated by summing over just $|Y_j|$ terms.

Imagine we are given $l = 1, \dots, N$ samples, $x^{(l)}$, drawn from unknown distribution $p(x)$. If x is very high dimensional, we do not want to enumerate over all possible values of x . Instead, we consider the quantity in Eq. 7 and Eq. 8 only for observed samples.

$$p(y|x^{(l)}) = \frac{1}{Z(x^{(l)})} p(y) \prod_{i=1}^n \left(\frac{p(y|x_i^{(l)})}{p(y)} \right)^{\alpha_{i,j}}$$

In log-space, this has an even simpler form.

$$\log p(y|x^{(l)}) = (1 - \sum_i \alpha_i) \log p(y) + \sum_{i=1}^n \alpha_i \log p(y|x_i^{(l)}) - \log Z(x^{(l)})$$

That is, the probabilistic label, y , for any sample, x , is a linear combination of weighted terms for each x_i . We recover $p(y|x)$ by doing a nonlinear transformation consisting of exponentiation and normalization.

The consistency requirements which are sums over the state space of x can be replaced with sample expectations.

$$p(y) = \sum_x p(x)p(y|x) \approx \frac{1}{N} \sum_{j=1}^N p(y|x^{(j)}),$$

with similar estimates for the marginals $p(y|x_i)$. In practice, to limit the complexity in terms of the number of samples, we can choose a random subset of samples at each iteration and estimate the probabilistic labels and marginals only for them. The details of the optimization over α are described in the next section.

Special case for Eq. 3 Note that the optimization in Eq. 3 corresponds to $j = 1, \dots, m$ with $m = 1$ and $\forall i, \alpha_i = 1$.

Convergence The updates for the iterative procedure described here are guaranteed not to decrease the objective at each step and are guaranteed to converge to a local optimum. Theoretical details are described elsewhere [8].

B Implementation Details for CorEx

As pointed out in Sec. 5, the objective in Eq. 6 (for a single Y_j) appears exactly as a bound on ‘‘ancestral’’ information [22]. We use this fact to motivate our choice for parameters in Eq. 9. Consider the soft-max function we use to define α^* .

$$\alpha_{i,j}^* = \exp \left(\gamma(I(X_i : Y_j) - \max_j I(X_i : Y_j)) \right)$$

First of all, we allow $\gamma_{i,j}$ to take different values at different i, j . We start by enforcing the form $\gamma_{i,j} = C_j/H(X_i)$. That way, the value of the exponent depends on normalized mutual information (NMI) instead of mutual information. The minimum value that can occur is $\exp(-C_j)$. We set $C_j = 1$. If the difference of NMI’s take the minimum value of -1 , we get $\alpha_{i,j}^* \sim 1/3$. According to the Steudel and Ay bound, X_i can still contribute to a non-negative value for the part of objective Eq. 6 that involves Y_j as long as X_i shares a common ancestor with at least $1/\alpha + 1$ other variables. At the beginning of the learning, this is desirable as it allows all Y_j ’s to learn significant structures even starting from small values of $\alpha_{i,j}$. However, as the computation progresses, we would like to force the soft-max function to get closer to the true hard max solution. To that end, we set $\gamma_{i,j} = (1 + D_j)/H(X_i)$, where $D_j = 500 \cdot |\mathbb{E}_X(-\log Z_j(x))|$. The D_j term represents the amount of correlation learned by Y_j [8]. For instance, if all $p(y_j|x_i) = p(y_j)$, $\log Z_j(x) = 0$ and Y_j has not learned anything. As the computation progresses and Y_j learns more structure, we smoothly transition to a hard-max constraint.

In all the experiments shown here, we set $|Y_j| = k = 2$. For convergence of Algorithm 1, we check when the magnitude of changes of $\mathbb{E}_X \log(-\sum_j Z_j(x))$ consistently falls below a threshold of 10^{-5} or when we reach 1000 iterations, whichever occurs first. We set $\lambda = 0.3$ based on several tests with synthetic data.

We construct higher order representation from the bottom up. After applying Algorithm 1, we take the most likely value of Y_j for each sample in the dataset. Then we apply CorEx again using these labels as the input. In principle, this sample of Y ’s does not accurately reflect $p(y) = \sum_x p(y|x)p(x)$ and a more nuanced approximation like contrastive divergence could be used. However, in practice it seems that CorEx typically learns nearly deterministic functions of x , so that the maximum likelihood labels well reflect the true distribution.

In Fig. 2, we suggested that uncorrelated random variables could be easily detected. In practice we used a threshold that this was the case if $MI(X_i : Y_{parent(X_i)})/min(H(X_i), H(Y)) < 0.05$. At higher layers of representation, this helps us identify root nodes. For the DNA example in Fig. 3, ‘‘gender’’ was a root node, but for visual simplicity all root nodes were connected at the top level. Following similar reasoning as above, we can also check which Y_j ’s have learned significant structure by looking at the value of $\mathbb{E}_X(-\log Z_j(x))$.

C Implementation Details for Comparisons

We represented the data from the binary erasure channel either as integers ($0[X_i = 0], 1[X_i = e], 2[X_i = 1]$) for methods that deal with categorical data, or as floating numbers on the unit interval for methods that require data of that form, ($0[X_i = 0], 0.5[X_i = e], 1[X_i = 1]$). In principle, we could also have treated “erased” information as missing. But we treated erasure as another outcome in all cases, including for CorEx.

CorEx naturally handles missing information (you can see that Eq. 7 can be easily marginalized to find labels even if some variables are missing). We had to use this fact for the DNA dataset which did have some SNPs missing for some samples. In fact, because CorEx is, in a sense, looking for the most redundant information, it is quite robust to missing information.

We will now briefly describe the settings for various learning algorithms learned. We used implementations of standard learning techniques in the scikit library for comparisons [34] (v. 0.14). We only used the standard, default implementation for k-means, PCA, ICA, and “hierarchical clustering” using the Ward method. For spectral clustering we used a Gaussian kernel for the affinity matrix and a nearest neighbors affinity matrix using 3 or 10 neighbors. For spectral bi-clustering we tried clustering either the data matrix or its transpose. We set the number of clusters to be m in the direction of variables and either 10 or 32 clusters for the variables. Note that the true number of clusterings in the sample space was 2^8 . For NMF we tried Projected Gradient NMF and NMF with the two types of implemented sparseness constraints. For the restricted Boltzmann machine, we used a single layer network with m units and learning rates 0.01, 0.05, 0.1. To cluster the input variables, we looked for the neuron with the maximum magnitude weight. For dimensionality reduction techniques like LLE and Isomap, we used either 3 or 10 nearest neighbors and looked for a m component representation. Then we clustered variables by looking at which variables contributed most to each component of the representation.

C.1 Twenty newsgroups

For the twenty newsgroups dataset, scikit has built-in function for retrieving and processing the dataset. We used the command below, resulting in a dataset with 18,846 posts. (Several different versions of this dataset are in circulation.)

```
sklearn.datasets.fetch_20newsgroups(subset='all',
                                    remove=('headers', 'footers', 'quotes'))
```

Because we are doing unsupervised learning, we combined the parts of the data normally split into training and testing sets. The attempt to strip footers turned out to be particularly relevant. The heuristic to do so looks for a single line at the end of the file, set apart from the others by a blank line or some number of dashes. Obviously, many signature lines fail to conform to this format and this resulted in strongly correlated signals. This led to features at layer 1 that were perfect predictors of authors, like Gordon Banks, who always included a quote: “Skepticism is the chastity of the intellect, and it is shameful to surrender it too soon.”

We considered any collection of upper or lower-case letters as a “word”. All characters were lower-cased. Apostrophes were removed (so that “I’ve” becomes “ive”). We considered the top ten thousand most frequent words. For the thousand most frequent words, for each document we recorded a 0 if the word was not present, 1 if it was present but occurred with less than the average frequency, or a 2 if it occurred with more than average frequency. For the remaining words we just used a 0/1 representation to reflect if a word was present.

CorEx details For the twenty newsgroups data, we trained CorEx in a top-down-bottom-up way. We started with a “low resolution” model with $m = 100$ hidden units and $k = 2$. We used the result of this optimization to construct 100 large groups of words. Then, for each (now much smaller) group of words, we applied CorEx again to get a more fine-grained representation (and then we discard the representation that we used to find the original clustering). The result was a representation at layer 1 with 326 variables. At the next layer we fixed $m = 50$, all units were used. At the next two layers we fixed $m = 10, 1$, respectively.

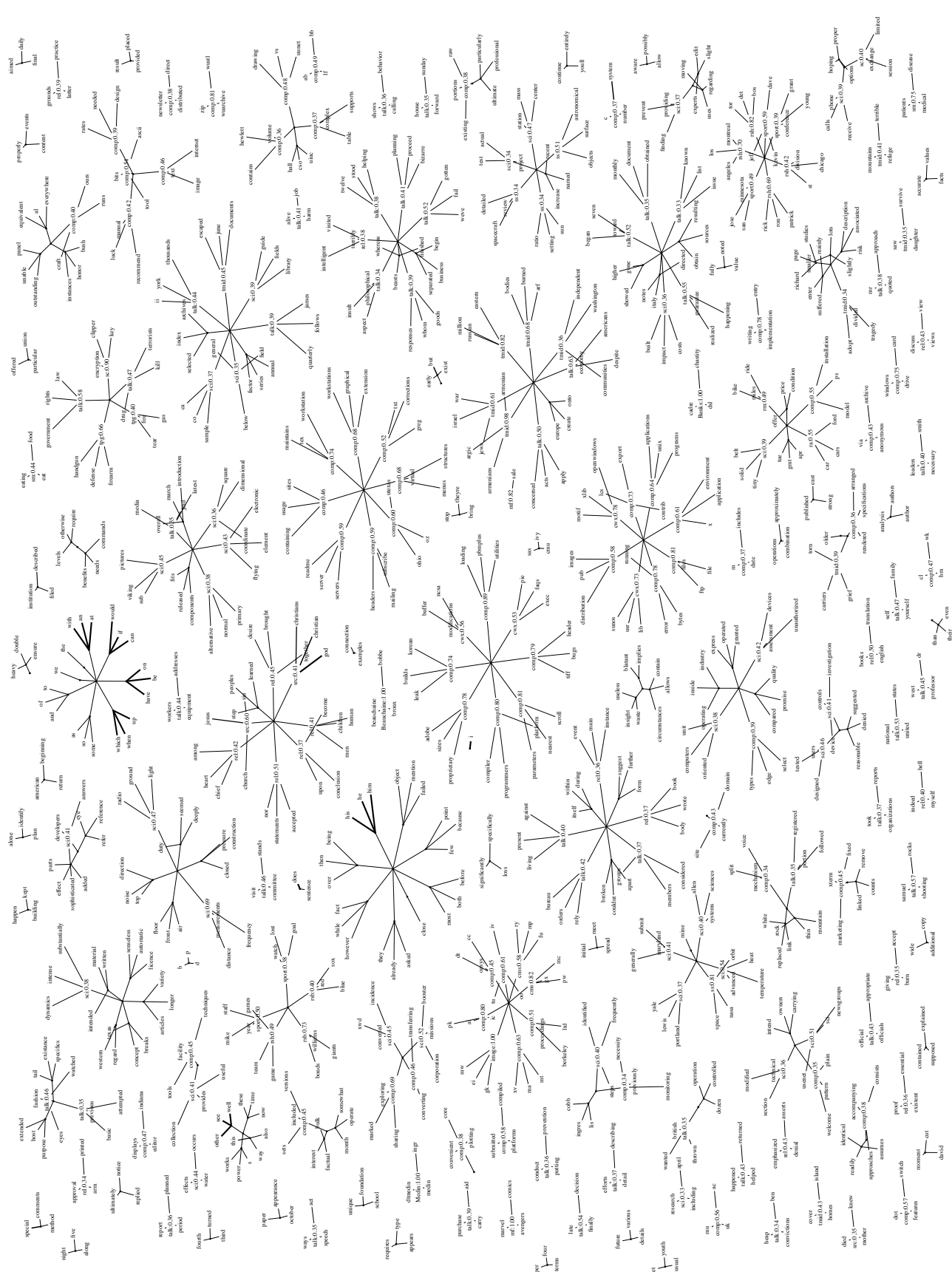


Figure C.1: The bottom three layers of the hierarchical representation learned for the twenty newsgroups dataset, keeping only the three leaf nodes with the highest normalized mutual information with their parents and up to eight branches per node at layer 2. For latent variables, we list an abbreviation of the newsgroup it best corresponds to along with the precision. For a zoomable version online go to <http://bit.ly/corexvis>.

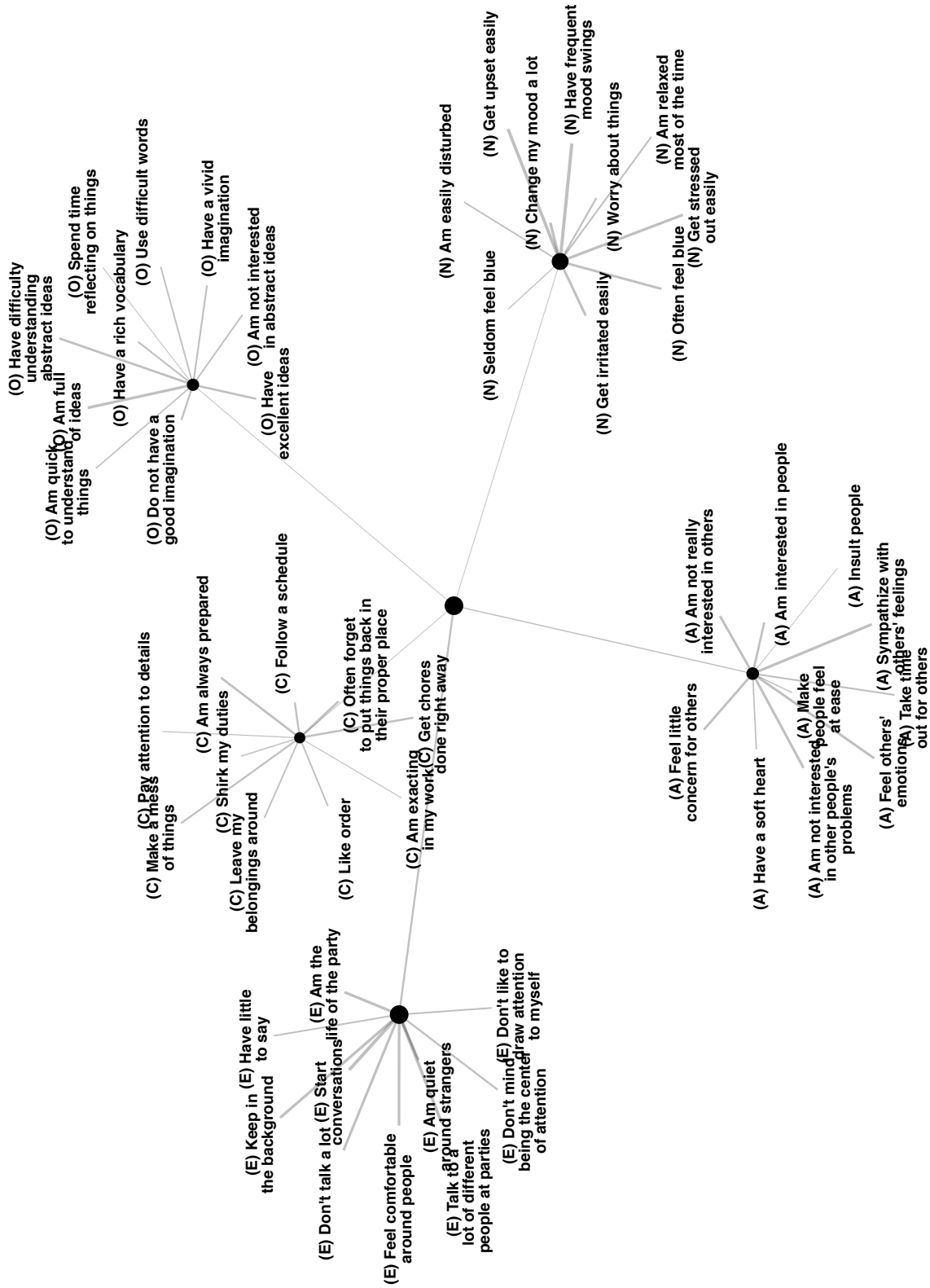


Figure C.2: CorEx learns a hierarchical representation from personality surveys with 50 questions. The number of latent nodes in the tree and number of levels are automatically determined. The question groupings at the first level exactly correspond to the “big five” personality traits. The prefix of each question indicates the trait test designers intended it to measure. The thickness of each edge represents mutual information between features and the size of each node represents the total correlation that the node captures about its children.